

# Benzalkonium Chloride Induces Dephosphorylation of Myosin Light Chain in Cultured Corneal Epithelial Cells

Ying Guo, Minati Satpathy, Graeme Wilson, and Sangly P. Srinivas

**PURPOSE.** Phosphorylation of myosin light chain (MLC) is essential for the contractility of the actin cytoskeleton, which regulates barrier integrity, adhesion, and migration. This study was conducted to investigate the effect of benzalkonium chloride (BAK), a preservative in topical ophthalmic formulations, on MLC phosphorylation in primary cultures of bovine corneal epithelial cells (BCECs).

**METHODS.** MLC phosphorylation was assessed by urea-glycerol gel electrophoresis followed by Western blot analysis. Activation of RhoA, which inhibits MLC phosphatase through Rho kinase, was examined by immunoprecipitation. The release of adenosine triphosphate (ATP) was measured by the luciferase-luciferin bioluminescence technique.

**RESULTS.** Positive expression of MLC kinase (MLCK) was found at the mRNA and protein levels by RT-PCR and Western blot analysis, respectively. Exposure to BAK for 10 to 20 minutes at concentrations of 0.0005%, 0.001%, and 0.003% reduced MLC phosphorylation by more than 30%. In addition, BAK led to thinning of the cortical actin and a decrease in cell adhesion. However, RhoA activity was found to increase with BAK treatment. Similar to BAK, ATP-depletion (induced by both antimycin-A and hypoxia) led to MLC dephosphorylation. BAK exposure also showed acute ATP release.

**CONCLUSIONS.** BAK induces acute ATP release and concomitant MLC dephosphorylation in bovine corneal epithelial cells. The dephosphorylation, presumably due to ATP loss, is indicative of a loss of contractility of the actin cytoskeleton that could affect cellular functions contributing to the maintenance of epithelial barrier integrity. (*Invest Ophthalmol Vis Sci.* 2007; 48:2001-2008) DOI:10.1167/iovs.06-0613

The cationic surfactant benzalkonium chloride (BAK) is a common disinfectant in topical ophthalmic formulations. Its concentration varies from 0.004% to 0.02%. BAK has poor penetration across the cornea and mostly accumulates in the epithelium.<sup>1</sup> Since the corneal epithelium forms a protective barrier on the ocular surface, any toxicity to the layer is damaging to the cornea. One major effect of BAK on the corneal epithelium is disruption of the barrier function.<sup>2-4</sup> Other adverse effects include accelerated cell desquamation,<sup>5,6</sup> compromised wound healing,<sup>7,8</sup> and cessation of mitosis.<sup>9</sup> However, the underlying mechanisms are not clear, although BAK

has been found to induce a variety of cellular changes such as cell membrane damage,<sup>10-12</sup> adenosine triphosphate (ATP) depletion,<sup>13</sup> generation of oxidative stress,<sup>14</sup> activation of AP-1 and NF- $\kappa$ B,<sup>15</sup> and cell apoptosis.<sup>16</sup>

The corneal epithelium undergoes a continuous self-renewal process to maintain its barrier integrity. The process involves continuous shedding of the superficial squamous cells followed by their replacement from deeper layers. Because mitotic activity occurs only in the basal epithelial cells, shedding of the superficial cells is balanced by cell proliferation and centripetal migration.<sup>17</sup> In other words, accelerated desquamation and/or inhibited mitosis or migration can lead to a loss of cells in the superficial layers and can thereby adversely affect the barrier integrity of the epithelium. Alternatively, the barrier integrity can be disrupted by a breakdown of the interactions of the transmembrane proteins of tight junctions as shown for corneal endothelial<sup>18</sup> and vascular endothelial monolayers.<sup>19</sup> The tethering forces, which are a prerequisite for interactions of the transmembrane proteins, are sensitive to contractility of the cortical actin cytoskeleton. When the tone of this peripheral actin is increased, a centripetal force opposing the tethering forces is generated, leading to a breakdown of the barrier integrity.<sup>19-21</sup> Since there is extensive involvement of actin contractility in the regulation of tight junctions, cell adhesion,<sup>22</sup> and motility,<sup>23,24</sup> we have examined the biochemical effects of BAK on the actin cytoskeleton in this study.

As in smooth muscle cells, contractility of the actin cytoskeleton in nonmuscle cells is regulated by phosphorylation of myosin light chain (MLC; 20 kDa). The extent of MLC phosphorylation is determined by two opposing pathways<sup>25,26</sup>: MLC kinase (MLCK)-driven phosphorylation and MLC phosphatase (MLCP)-driven dephosphorylation. MLCK is a dedicated kinase for phosphorylating MLC and is activated when bound to the Ca<sup>2+</sup>-calmodulin complex. MLC is dephosphorylated by MLCP, a heterotrimeric complex consisting of the catalytic subunit (PP1c $\delta$ ; 38 kDa), the myosin binding subunit (MYPT1; 130 kDa), and a small subunit of unknown function (M20; 20 kDa). Phosphorylation of MYPT1 by Rho kinase (at Thr-696 and Thr-850 residues) inhibits the phosphatase activity of PP1c $\delta$ .<sup>27-29</sup> Rho kinase is an effector molecule for the small GTPase, RhoA. The RhoA-Rho kinase axis is well known to be activated in response to G protein-coupled receptors (GPCRs) coupled to G $_{\alpha 12/13}$  G proteins.<sup>30</sup> PKC inactivates MLCP through phosphorylation of CPI-17 (the PKC-activated 17-kDa inhibitor protein of type 1 phosphatase; 17 kDa), which is known to inactivate PP1c $\delta$ .<sup>26</sup> Thus, activation of Rho kinase and/or PKC results in contraction of the actin cytoskeleton.

To date, there have been no studies on MLC-regulated actin contractility in corneal epithelial cells. Examination of MLC phosphorylation in response to BAK may not only help ascertain the molecular mechanisms underlying the epithelial effects of the preservative, but may also bring forward the significance of actin contractility in maintenance of the barrier integrity of the epithelium.

From the School of Optometry, Indiana University, Bloomington, Indiana.

Supported by National Eye Institute Grant EY14415 (SPS) and by a Faculty Research Support Program award from the Office of the Vice Provost for Research at Indiana University.

Submitted for publication June 6, 2006; revised November 20, 2006; accepted March 16, 2007.

Disclosure: Y. Guo, None; M. Satpathy, None; G. Wilson, None; S.P. Srinivas, None

The publication costs of this article were defrayed in part by page charge payment. This article must therefore be marked "advertisement" in accordance with 18 U.S.C. §1734 solely to indicate this fact.

Corresponding author: Sangly P. Srinivas, 800 East Atwater Avenue, Indiana University, School of Optometry, Bloomington, IN 47405; srinivas@indiana.edu.

## MATERIALS AND METHODS

### Drugs and Chemicals

Bovine calf serum (BCS) was purchased from Hyclone (Logan, UT). All other cell culture supplies were from Invitrogen-Gibco (Grand Island, NY). Bovine  $\alpha$ -thrombin and Y-27632 were purchased from Calbiochem (La Jolla, CA) and Tocris (Ballwin, MO), respectively. Enhanced chemiluminescence reagent was purchased from GE Healthcare (Piscataway, NJ). Phalloidin conjugated to Texas red was obtained from Invitrogen-Molecular Probes (Eugene, OR). All other drugs and reagents were purchased from Sigma-Aldrich (St. Louis, MO).

### Primary Culture of Bovine Corneal Epithelial Cells (BCECs)

Bovine eyes from a local abattoir were delivered on ice and disinfected with 1% iodine. Corneal epithelium, along with a small thickness of stroma, was dissected using a scalpel and incubated in 2 U/mL Dispase at 37°C for 90 minutes. Epithelial sheets were then removed under a dissection microscope and incubated further at 37°C in 0.05% trypsin. After 15 minutes, trypsin was deactivated by exposure to a growth medium containing 10% BCS. Cells were then collected by centrifugation. After the supernatant was discarded, cells were resuspended in DMEM/F12 culture medium supplemented with 10% BCS, 5  $\mu$ g/mL insulin, 5 ng/mL epidermal growth factor, and an antibiotic-antimycotic mixture (50  $\mu$ g/mL gentamicin and 50 ng/mL amphotericin B). Cells were cultured at 37°C in a humidified atmosphere containing 5% CO<sub>2</sub> and 95% air. The medium was replaced on alternate days. The second- and third-passage cells were used for all experiments.

### RT-PCR Assays

Total RNA was isolated from bovine corneal cells (BCECs; Trizol; Invitrogen-Gibco) and quantified by absorption at 260 nm. First-strand cDNA was synthesized for RT-PCR (SuperScript III Reverse Transcriptase; Invitrogen-Gibco). Sequences used for the primers used for MLCK are 5'-ATGAAGTTCGAAAGCAGATCC-3' (forward [F]) and 5'-GTGGTG-GAGGCAGTTCATGATG-3' (reverse [R]). For RhoA, the primer sequences are 5'-TGGCTGCCATCCGGAAGAACT-3' (F) and 5'-AGATC-CTTCTGTTCCTCAACCAG-3' (R); and for Rho kinase I, the sequences are 5'-GTGCAATTGGAGAAGTCAATTGG-3' (F) and 5'-CAAGTAC-CAAAATCTGCTAACTTCA-3' (R). RT-PCR products were run on an agarose gel (1%) and visualized by ethidium bromide staining along with 100-bp and 1000-bp ladder molecular mass markers (GE Healthcare).

### Expression of MLCK by Western Blot Analysis

A monoclonal antibody directed against chicken gizzard MLCK (K36; 1:5000), known to recognize human, bovine, and avian MLCK (both smooth muscle and vascular endothelial isoforms) was used. Cells grown on Petri dishes were lysed with an ice-cold lysis buffer containing 50 mM Tris-HCl (pH 7.6), 150 mM NaCl, 1% Triton X-100, 2 mM EGTA (pH 8.0), EDTA, dithiothreitol (DTT), phenylmethylsulfonyl fluoride (PMSF), NaF, and a protease inhibitor cocktail (containing leupeptin, pepstatin, chymostatin, and aprotinin). After a preclearing centrifugation step (14,000 rpm for 15 minutes at 4°C), the whole lysate was subjected to SDS-PAGE (100  $\mu$ g protein/lane) and immunoblot analysis. Membranes were blocked with TBST containing 5% nonfat dry milk for 1 hour at room temperature (RT), and subsequently incubated with the primary antibody that had been diluted in TBST and dry milk overnight at 4°C. Blots were washed with TBST for three times (15 minutes each) and then visualized using the peroxidase-conjugated secondary antibody and chemiluminescence (ECL; GE Healthcare).

### Quantitative Estimation of MLC Phosphorylation

MLC phosphorylation was assayed by using urea-glycerol electrophoresis and Western blot analysis, as previously described.<sup>31</sup> In brief, cells

grown on 60-mm Petri dishes were exposed to different drugs before protein was extracted with a urea sample buffer and subjected to electrophoresis. The separated phosphorylated MLC and nonphosphorylated MLC were detected by Western blot analysis with a specific anti-MLC antibody (E201; 1:3000). Scanned images of the bands were quantified by using a custom-made software program. The migration speeds of the mono- (P) and di- (PP) phosphorylated MLC and the nonphosphorylated (NP) form of MLC are as follows: PP > P > NP. The pixel intensity of each band was quantified by densitometry, and the fraction of p-MLC was calculated by dividing the total p-MLC (equal to the sum of P + PP) by total MLC (given by P + PP + NP). Treatment with thrombin was used as a positive control, since its effects on MLC phosphorylation are well understood.<sup>32-35</sup>

### Staining of Actin Cytoskeleton

BCECs grown on glass coverslips were washed with PBS after drug treatment, fixed for 10 minutes with 3.7% paraformaldehyde/PBS, and permeabilized for 5 minutes with 0.2% Triton X-100/PBS. Cells were then incubated with Texas red-conjugated phalloidin (1:500; Invitrogen-Molecular Probes) in the dark for 45 minutes at RT. Coverslips were mounted with an antifade agent containing *p*-phenylenediamine (Invitrogen-Molecular Probes) and viewed by fluorescence microscopy ( $\lambda_{\text{ex}} = 542$  nm and  $\lambda_{\text{em}} = 563$  nm).

### Adhesion Assay

Ninety-six-well tissue culture plates were coated with a mixture of 10  $\mu$ g/mL fibronectin and 35  $\mu$ g/mL collagen I (AthenaES, Baltimore, MD). BCEC ( $1 \times 10^5$  cells) suspended in serum-free DMEM/F12 were then plated and allowed to attach for 90 minutes at 37°C. Nonadherent cells were removed by gently washing four times with 200  $\mu$ L growth medium. Attached cells were detected by incubating with 0.6  $\mu$ M calcein-AM (Vybrant cell adhesion assay kit; Invitrogen-Molecular Probes) for 30 minutes at 37°C. The dye is hydrolyzed to hydrophilic calcein that is retained in viable cells. The number of cells was quantified as fluorescence of calcein measured with a microplate reader ( $\lambda_{\text{ex}} = 494$  nm and  $\lambda_{\text{em}} = 517$  nm; FLUOstar; BMG, Offenburg, Germany).

### RhoA Activation Assay

An absorbance-based ELISA technique (RhoA G-LISA kit; Cytoskeleton, Denver, CO) was used to quantify the effect of BAK. Cells in 60-mm Petri dishes first received 0.5% serum treatment for 24 hours and were then serum-starved for 16 to 18 hours before drug treatment. RhoA-GTP in cell lysate was allowed to bind to the wells coated with a Rho-GTP-binding protein for 30 minutes. Inactive RhoA-GDP was removed by agitated washing. Bound RhoA-GTP was detected with a RhoA-specific antibody and an HRP-labeled secondary antibody. After the reaction was stopped, absorbance was measured at 490 nm with a spectrophotometer (DU-64; Beckman Coulter, Fullerton, CA).

### ATP Release Assay

ATP release was assessed in real-time using the luciferase-luciferin (LL) bioluminescence technique. The luminometer was custom built around a cooled photomultiplier tube (H7422P-40; Hamamatsu Inc., Bridgewater, NJ). Cells grown on 35-mm Petri dishes and bathed in 600  $\mu$ L medium (Opti-MEM I; Invitrogen-Gibco) containing 4 mg/mL LL were placed in proximity to the cathode of the photomultiplier. The luminescence emitted on ATP release and the subsequent oxidation of luciferin, passed through the bottom of the Petri dish to the cathode of the photomultiplier. The output of the photomultiplier in the form of voltage pulses was counted by a high-speed (80 MHz) timer-counter interface in a PC (NI-6602; National Instruments, Austin, TX). Independent calibration experiments in cell-free Petri dishes showed a linear increase in luminescence count with increasing ATP content over four orders of magnitude ( $10^{-13}$ - $10^{-9}$  moles; 66 counts/picomole;  $r = 0.99$ ).

## Flow Cytometry Analysis of Cell Death

An annexin V-FITC apoptosis kit (BioVision; Mountain View, CA) was used to detect dead cells. After treatment with BAK, cells were trypsinized and incubated in dark for 5 minutes with annexin V-FITC (1:250). Next, the cells were washed with annexin-binding buffer followed by incubation with propidium iodide (PI; 1:250) in dark for 5 minutes. Annexin V detects apoptotic cells by binding to phosphatidylserine (PS), which translocates to the outside surface of the plasma membrane during early stages of apoptosis. Propidium iodide penetrates into the cells, in which the plasma membrane is damaged, usually an indication that cells are undergoing necrosis. All measurements were performed on a flow cytometer (FACScan; BD Biosciences, San Jose, CA) using the system software for data analysis (CellQuest Pro; BD Biosciences). For each sample, at least 10,000 events were analyzed.

## Data Analysis

Data were analyzed by one-way ANOVA with the Bonferroni test for posttest analysis (Prism 4.0 for Windows; GraphPad Software Inc., San Diego, CA). For the G-LISA assay of RhoA activity, results were analyzed by using the paired *t*-test.  $P < 0.05$  was considered statistically significant.

## RESULTS

### Expression of MLCK, RhoA, and Rho Kinase in BCECs

As the first step to characterize MLC phosphorylation in BCECs, we determined expression of MLCK, RhoA, and Rho kinase. RT-PCR showed a positive band at the expected band size of 740 bp for the transcript of MLCK (Fig. 1A). The corresponding protein expression was confirmed by Western blot analysis, as shown in Figure 1B (Epi). The band at 220 kDa corresponds to the vascular endothelial isoform of MLCK (EC-MLCK; 220 kDa). It is noteworthy that the corneal endothelial cells used as a positive control showed expression of both the smooth muscle (SM-MLCK; 130 kDa) and EC-MLCK isoforms (Endo).

Transcripts of the small GTPase RhoA and its downstream effector Rho kinase I at the mRNA level are also found in BCECs. Figure 1A shows expected bands at 361 bp and 405 bp, corresponding to transcripts of RhoA and Rho kinase I, respectively.

### Effect of BAK on MLC Phosphorylation

To secure functional evidence for MLCK, RhoA, and Rho kinase, we examined the response of BCECs to the protease activated receptor (PAR)-1 agonist, thrombin. PAR-1 receptors, coupled to  $G_{\alpha 12/13}$  G protein, mobilize the RhoA-Rho kinase axis.<sup>36</sup> This has been demonstrated in BCECs in one of our recent studies.<sup>31</sup> As shown in Figure 2, when epithelial cells were exposed to thrombin (2 U/mL; 2 minutes), a significant

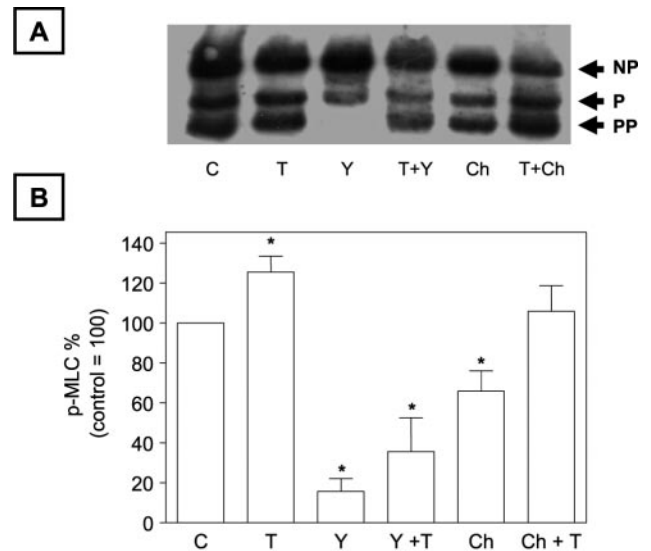
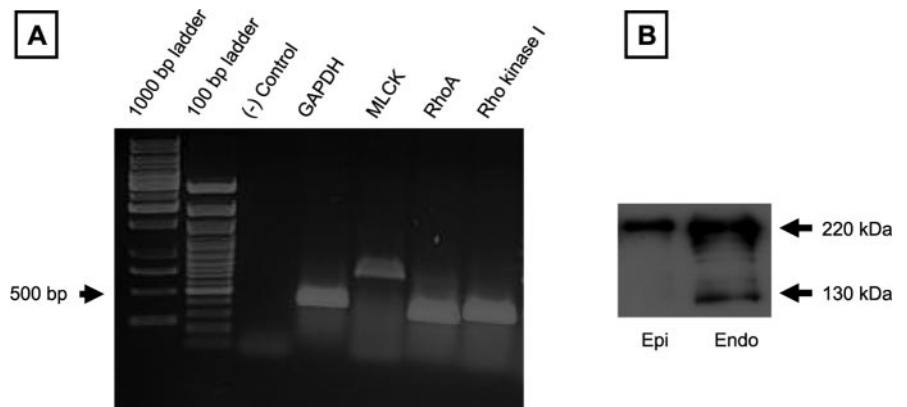


**FIGURE 2.** Thrombin-induced MLC phosphorylation in BCECs. The cells were exposed to thrombin (2 U/mL, 2 minutes) and then were subjected to urea glycerol gel electrophoresis followed by Western blot analysis. (A) A typical gel showing thrombin-induced MLC phosphorylation (lane T) which was inhibited by Y-27632 (10  $\mu$ M, 30 minutes; lane T+Y) and chelerythrine (10  $\mu$ M, 10 minutes; lane T+Ch). BCECs showed a basal level of MLC phosphorylation under control conditions (lane C). Both Y-27632 and chelerythrine inhibit this basal MLC phosphorylation (lanes Y, Ch). (B) A summary of the densitometric analysis of the thrombin response. \*Significant difference from the control. C, control; T, thrombin; Y, Y-27632; Ch, chelerythrine.

increase in p-MLC (125.6%,  $n = 5$ ) was noticed. Cells also showed a significant level of MLC phosphorylation under basal conditions (Fig. 2A; C). The thrombin response was inhibited by pre-exposure to the Rho kinase inhibitor, Y-27632 (10  $\mu$ M; 30 minutes; p-MLC = 35.6%,  $n = 4$ ) or the PKC inhibitor, chelerythrine (10  $\mu$ M; 10 minutes; p-MLC = 103.9%,  $n = 4$ ). These inhibitors also reduced the basal level of MLC phosphorylation (Y-27632, 15.7%,  $n = 4$ ; chelerythrine, 65.8%,  $n = 4$ ). A summary plot of these findings is shown in Figure 2B. These results, taken together, not only provide functional evidence for RhoA-mediated MLC phosphorylation in BCECs for the first time, but also establish the MLC assay protocol.

Using the same protocol, we next examined the effect of BAK on MLC phosphorylation on its exposure for 10, 20, and 30 minutes. A typical urea-glycerol gel obtained in response to 0.003% BAK is shown in Figure 3A. As summarized in Figure 3B, 0.003% BAK caused MLC dephosphorylation by  $53\% \pm 10\%$

**FIGURE 1.** Expression of MLCK in cultured BCECs. (A) RT-PCR analysis showed a positive band at the expected size for MLCK (740 bp). Transcripts of RhoA and Rho kinase I were also found at the expected sizes of 361 and 405 bp, respectively. GAPDH was the positive control (430 bp). (B) Western blot analysis indicated expression of the EC isoform of MLCK (220 kDa) in BCEC. Epi, epithelial cells; Endo, endothelial cells.



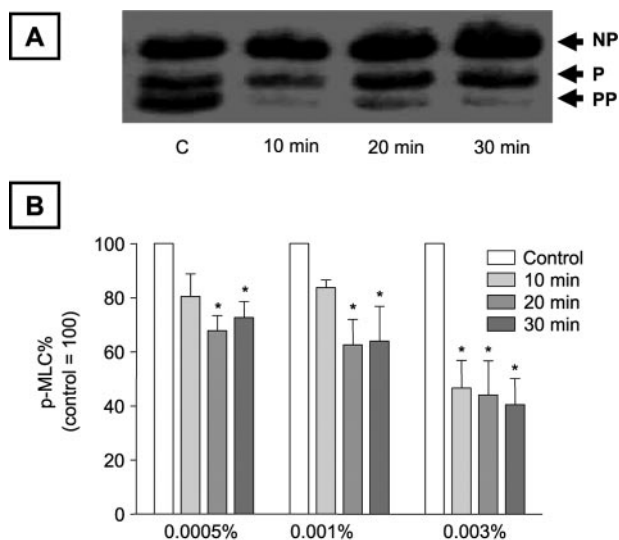


**FIGURE 3.** Dephosphorylation of p-MLC in response to BAK. Cells were exposed to BAK at different concentrations (0.0005%, 0.001%, and 0.003%) for different exposure time. (A) A representative urea-glycerol gel showing significant MLC dephosphorylation at 10, 20, and 30 minutes induced by 0.003% BAK. (B) A summary plot of the densitometric analysis of the BAK response. \*Significant difference from the control of the group ( $P < 0.05$ ).

( $n = 5$ ) within 10 minutes. The dephosphorylation was 60% at 30 minutes ( $60\% \pm 10\%$ ;  $n = 5$ ). At lower concentrations, BAK caused relatively reduced dephosphorylation. At 10 minutes, there was no significant effect at the concentrations of 0.001% or 0.0005% ( $P > 0.05$ ). However, at 20 minutes, MLC dephosphorylation was significantly different from the control (0.001% BAK:  $37\% \pm 9\%$ ,  $n = 6$ ; and 0.0005% BAK:  $32\% \pm 6\%$ ,  $n = 6$ ), and this lasted for at least 30 minutes ( $36\% \pm 13\%$  for 0.001% BAK and  $27\% \pm 6\%$  for 0.0005% BAK;  $n = 6$ ).

### Effect of BAK on Actin Cytoskeleton

MLC phosphorylation promotes actomyosin interaction<sup>37</sup> and actin reorganization.<sup>38</sup> In corneal endothelium, MLC phosphorylation led to disruption of cortical actin and development of interendothelial gaps.<sup>31</sup> We examined organization of the actin cytoskeleton in response to BAK using phalloidin (conjugated to Texas Red) staining. The untreated cells showed a dense web of cortical actin (Fig. 4A), which has often been referred to as the perijunctional actomyosin ring (PAMR).<sup>21,31,39</sup> BAK,

at the concentration of 0.001%, caused thinning of the cortical actin bundles (Fig. 4B). The effect became more prominent at 0.003% (Fig. 4C).

### Effect of BAK on Cell Adhesion

Reduced actin contractility is known to cause loss of integrin-mediated focal adhesion of cells.<sup>40,41</sup> Consistent with MLC dephosphorylation, which indicates a decrease in actin contractility, BAK induced a significant reduction in cell adhesion. As shown in Figure 5, coating of culture plates with a cocktail of fibronectin and collagen I increased cell adhesion by 28% ( $n = 10$ ;  $P < 0.001$ ). However, even with coating, cell adhesion was reduced by 42% ( $n = 10$ ,  $P < 0.001$ ) in response to 0.001% BAK. No effect of BAK was found at 0.0001% ( $n = 10$ ;  $P > 0.05$ ).

### Effect of BAK on RhoA

Since the RhoA-Rho kinase axis plays a key role in MLC phosphorylation and consequently in the regulation of actin cytoskeleton at focal adhesions,<sup>22</sup> we examined RhoA activity with BAK treatment. The immunoprecipitation results showed negligible RhoA activity in serum-starved control cells (Fig. 6, Control). Thrombin (2 U/mL; 2 minutes), used as a positive control, caused a 1.5-fold increase ( $n = 5$ ,  $P < 0.05$ ) in RhoA activity (Fig. 6, T). Instead of the inhibition of RhoA, as suggested by MLC dephosphorylation data (Fig. 3), 0.001% BAK led to a 1.8-fold increase in RhoA activity ( $n = 5$ ,  $P < 0.05$ ; Fig. 6, BAK). No additive effect was seen with cotreatment of BAK and thrombin.

### ATP Release Induced by BAK

BAK is known to cause ATP depletion in corneal epithelial cells. However, effect has been reported only at the high concentration of 0.01%,<sup>13</sup> and the underlying mechanism has not been explored. Accordingly, we examined ATP release in real-time at lower concentrations of BAK, by using the luciferase-luciferin bioluminescence technique. As shown in Figure 7A, both 0.001% and 0.003% BAK caused a precipitous increase in the luminescence count. The luminescence signal declined exponentially after the peak but lasted at least for several minutes. The peak ATP release averaged  $65 \pm 19$  nM ( $n = 15$ ) with 0.001% BAK and  $102 \pm 16$  nM ( $n = 15$ ) with 0.003% BAK, as summarized in Figure 7B.

### MLC Phosphorylation on ATP Depletion

Since BAK led to an acute loss of intracellular ATP concomitant with MLC dephosphorylation, we examined MLC phosphory-

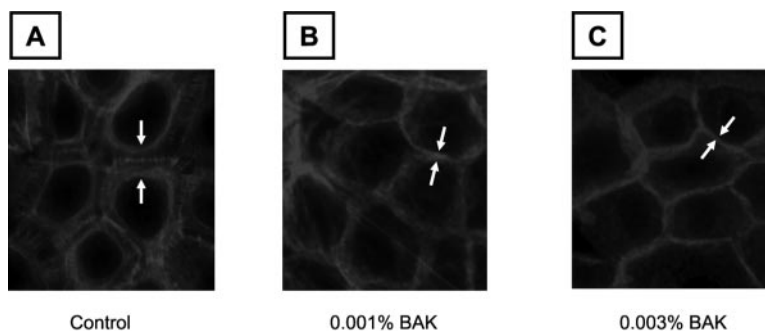


**FIGURE 4.** BAK-induced alteration of the cortical actin cytoskeleton. After BAK treatment for 30 minutes, cells were fixed and stained with Texas red phalloidin. The images are representative of at least three independent experiments. (A) Organization of the actin cytoskeleton labeled with phalloidin in the cortical cytoplasm (formation of PAMR) in untreated cells. (B) Exposure to 0.001% BAK for 30 minutes caused thinning of the cortical actin bundles. (C) Disruption of the cortical actin bundles with treatment of 0.003% BAK for 30 minutes. *Arrows:* thickness of the cortical actin cytoskeleton.

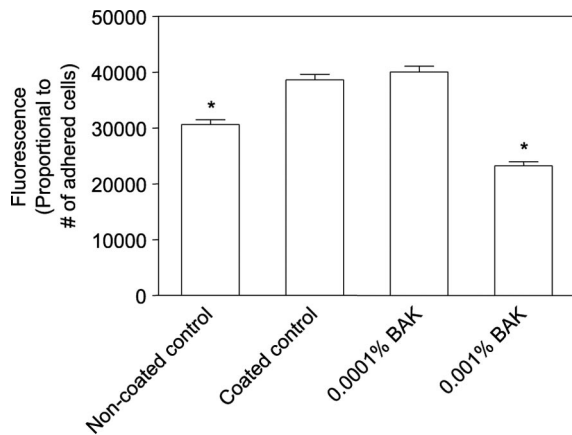


**FIGURE 5.** Reduced cell adhesion in the presence of BAK. Coating of fibronectin and collagen I significantly enhanced cell adhesion ( $P < 0.001$ ) compared to the noncoated control. BAK, at 0.001%, caused a remarkable reduction of cell adhesion ( $P < 0.001$ ) even with coating. BAK did not affect cell adhesion at a concentration of 0.0001% ( $P > 0.05$ ). \*Significant difference from the coated control.

lation in ATP-depleted cells to determine any causal relationship between the two. Cells were deliberately depleted of the intracellular ATP by inhibition of the oxidative phosphorylation with antimycin A (10  $\mu$ M; 10 minutes)<sup>42</sup> or hypoxia (1.5% O<sub>2</sub>; 180 minutes). The results (Fig. 8) show that both treatments brought about MLC dephosphorylation to a similar level (antimycin A: 44%  $\pm$  10%,  $n = 12$ ,  $P < 0.01$ ; hypoxia: 39%  $\pm$  4%,  $n = 5$ ,  $P < 0.05$ ).

### Effect of BAK on Cell Viability

To exclude the possibility that the effects of BAK were caused merely by cell death, cell viability was measured using flow cytometry by double staining with Annexin V and PI. The ratios of early apoptotic, late apoptotic, or necrotic cells to the total cells are shown in Figure 9. In control cells, a fraction of the population undergoes apoptosis and necrosis (0.93%  $\pm$  0.28% for early apoptosis, 0.85%  $\pm$  0.15% for apoptosis, and 2.45%  $\pm$  0.39% for necrosis). Staurosporine (STS), a potent nonselective protein kinase inhibitor and apoptosis inducer used as a positive control (17  $\mu$ M; 17 hours) significantly increased the ratio of early apoptotic (2.51%  $\pm$  0.46%;  $n = 6$ ,  $P < 0.05$ ) and fully apoptotic cells (2.15%  $\pm$  0.36%;  $n = 6$ ,  $P < 0.05$ ). At concentrations of 0.0005%, 0.001%, and 0.003%, BAK caused no apparent death of cells at 30 minutes ( $n = 6$  for each,  $P > 0.05$ ).

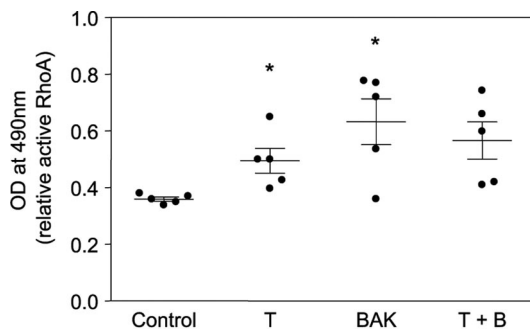


**FIGURE 6.** Effect of BAK on RhoA activity. Cells were serum-starved for 48 hours before being subjected to drug treatment and the ELISA assay. Both thrombin and BAK induced RhoA activation. No additive effect was found with cotreatment of the two drugs. T, thrombin; B, BAK. \*Significant difference from the control ( $P < 0.05$ ).

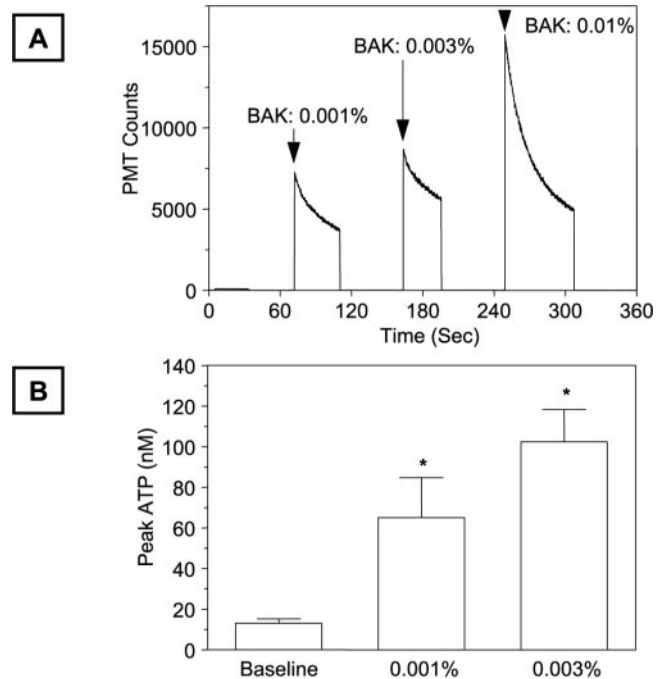


**FIGURE 7.** ATP release in response to BAK. Monolayers of BCEC were bathed in 600  $\mu$ L reduced-serum medium, which contained 4 mg/mL luciferase-luciferin. The luminescence measured is proportional to the amount of ATP released into the bathing medium. (A) Exposure to BAK caused a precipitous increase in luminescence. PMT: photomultiplier tube. (B) Summary of the peak ATP release induced by BAK. \*Significant difference from the baseline level ( $P < 0.001$ ).

### DISCUSSION

BAK is a widely used preservative in topical ophthalmic formulations, and its side effects on the cornea have been frequently investigated.<sup>43</sup> In this study, our main goal was to understand the molecular mechanisms by which BAK induces a loss in the barrier integrity of the corneal epithelium. Our principal finding is that BAK, at subclinical concentrations, induces significant MLC dephosphorylation in cultured BCECs. Since phosphorylated MLC induces actomyosin interaction,<sup>37</sup> BAK's effect is indicative of a loss in contractility of the actin cytoskeleton. In terms of cell biological activities, this implies that BAK could affect cell adhesion, cell movement, and division, as these activities are intricately coupled to the contractility of the actin cytoskeleton.<sup>22-24</sup> Furthermore, since the barrier integrity of the corneal epithelium is influenced by cell adhesion, cell movement, and proliferation, as per the XYZ hypothesis,<sup>17</sup> we suggest that the side effects of BAK can be traced to a compromised actin cytoskeleton.

### Contractility of the Actin Cytoskeleton

Our recent studies in corneal endothelium have demonstrated a disruption of the barrier integrity as a result of increased actin contractility in response to inflammatory agonists.<sup>31</sup> This was attributed to a loss of the intercellular tethering forces that maintain interactions of the transmembrane proteins at tight junctions. In the absence of such interactions, occlusion of the paracellular space is prevented and a loss of the barrier integrity becomes inevitable. The loss of the intercellular tethering forces, per se, is due to an increase in the contractility of the cortical actin cytoskeleton (PAMR, see Fig. 4A) which results in a net centripetal force.

Given that BAK is well known to induce a loss in the barrier integrity of the corneal epithelium, it was intriguing to deter-

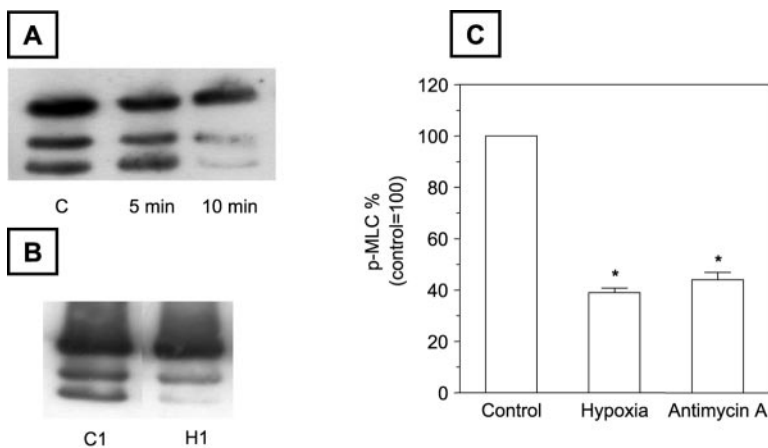


**FIGURE 8.** MLC dephosphorylation induced by deliberate ATP depletion. Cells were treated with antimycin (10  $\mu$ M) or hypoxia (1.5% O<sub>2</sub>, 3 hours) before subjected to MLC phosphorylation analysis. Both treatments induced significant MLC dephosphorylation. (A) A representative urea-glycerol gel showing MLC dephosphorylation induced by antimycin A. (B) A representative gel showing MLC dephosphorylation induced by hypoxia. (C) A summary plot of the densitometric analysis of the experiments similar to those shown in (A) and (B). \*Significant difference from the control (for antimycin A,  $P < 0.01$ ; for hypoxia,  $P < 0.05$ ).

mine whether the preservative affected MLC phosphorylation and actin contractility. We examined phosphorylation of MLC using a protocol involving urea-glycerol gel electrophoresis for separating the phosphorylated and nonphosphorylated forms of MLC followed by Western blot analysis for identification. This protocol has been established in our previous studies on corneal endothelial cells.<sup>31</sup> Since there have been no reports on MLC phosphorylation in corneal epithelial cells, we used thrombin as a positive control. It is known to induce MLC phosphorylation in corneal endothelial cells through G<sub>α12/13</sub> G protein-coupled PAR-1 receptors, which activates the RhoA-Rho kinase axis.<sup>31</sup> Consistent with the presence of PAR-1 receptors in corneal epithelial cells,<sup>44</sup> we observed significant MLC phosphorylation after treatment with thrombin (Fig. 2). In addition, we examined the expression of MLCK, RhoA, and Rho kinase. The positive results (Fig. 1) support the thrombin-induced MLC phosphorylation observed in BCECs (Fig. 2). It is worth noting that MLCK showed a differential expression of its two isoforms in corneal epithelial cells compared with corneal endothelial cells (Fig. 1B). Only the versatile EC-MLCK, which is the vascular endothelial isoform susceptible to modulation by several protein kinases,<sup>26,45</sup> was found in the epithelial cells.

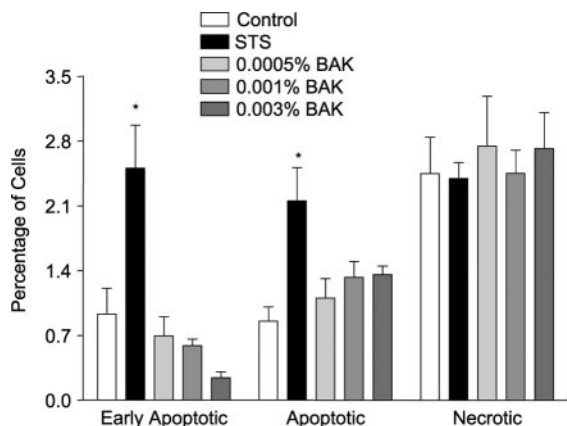


**FIGURE 9.** Flow cytometric analysis of cell death. The control cells have a fractional population of early apoptotic, apoptotic, and necrotic cells. Exposure to staurosporine (STS) at 17 nM for 17 hours increased the number of early apoptotic cells and fully apoptotic cells. No significant apoptosis or necrosis was found with treatment of BAK at concentrations of 0.0005%, 0.001%, and 0.003% within 30 minutes ( $P > 0.05$ ). \*Significant difference from the control ( $P < 0.05$ ).

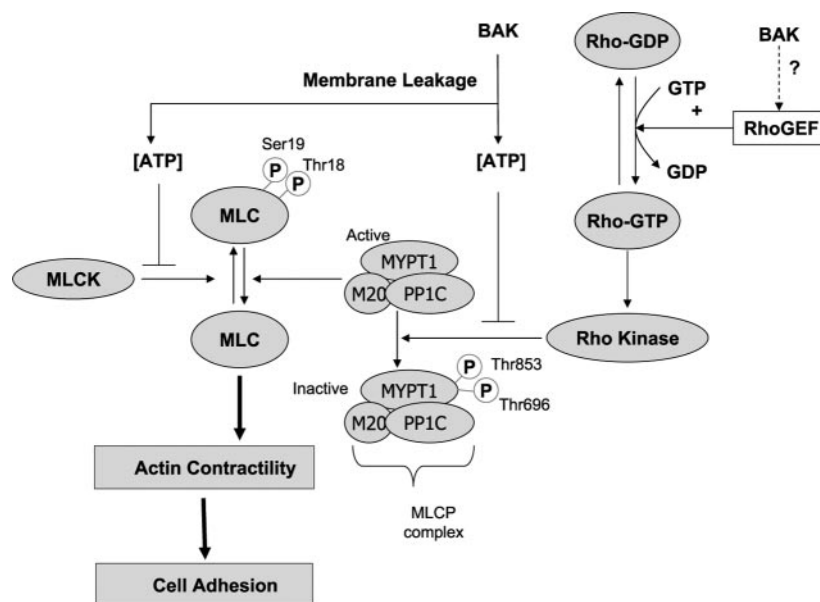
### Effects of BAK on the Actin Cytoskeleton

Applying the same protocol as for thrombin, we next examined the status of MLC phosphorylation in response to BAK at several subclinical concentrations. At all the concentrations examined, BAK consistently induced MLC dephosphorylation at the different time points of observation (Fig. 3), without causing significant cell death (Fig. 9). This finding suggests that the loss of barrier integrity caused by the preservative is not through increased actin contractility. Despite this unexpected finding, BAK induced two other significant effects related to the actin cytoskeleton concomitantly with MLC dephosphorylation: thinning of the cortical actin (Fig. 4) and loss of cell adhesion (Fig. 5). These effects are similar to what has been reported in response to ATP depletion in other epithelial cell types.<sup>42</sup> The thinning of the cortical actin, presumably due to severing and depolymerization of the actin filaments, may have significant impact on the intercellular tethering forces or the barrier integrity. The cortical actin is known to attach to a variety of linker proteins at the tight and adherence junctions.<sup>46</sup> Thus, a treatment with cytochalasin, an actin-severing-disrupting drug is known to affect the tight junction complex and consequently break down epithelial permeability.<sup>47-49</sup> Similarly, it is plausible that the loss of actin filaments in response to BAK contributes to a disintegration of the molecular assembly at the junctional complexes, resulting in a breakdown of the barrier integrity of the corneal epithelium.

### Mechanisms Contributing to MLC Dephosphorylation

MLC phosphorylation is positively influenced by Ca<sup>2+</sup>-dependent MLCK activity and negatively by Ca<sup>2+</sup>-independent MLCP (Fig. 10). Therefore, our observation that BAK induces RhoA activation concomitantly with MLC dephosphorylation is unexpected. The observed RhoA activation, however, can be attributed to the release of RhoGEFs as a result of BAK-induced direct activation of G proteins through nonspecific interactions during membrane damage,<sup>43,50</sup> production of ROS,<sup>14,51</sup> and membrane depolarization through activation of nonselective cation channels.<sup>52</sup> Many G proteins are known to mediate RhoA activation via RhoGEFs. ROS is also implicated in the release of RhoGEFs through microtubule depolymerization.<sup>28,53-55</sup> Although depolarization of the membrane potential is known to induce RhoA-Rho kinase-dependent disruption of actin cytoskeleton,<sup>56</sup> the mechanism for concomitant release of RhoGEFs is not known. Thus, leaving out inhibition of RhoA as a potential mechanism, we can attribute BAK-induced MLC dephosphorylation to either inhibition of MLCK

**FIGURE 10.** Cell signaling around MLC phosphorylation. Phosphorylation of MLC, which indicates increased actin contractility, is catalyzed by the  $\text{Ca}^{2+}$ -dependent MLCK. This effect is opposed by MLCP-driven dephosphorylation of MLC. The activity of MLCP is inhibited by RhoA-GTP through its downstream effector, Rho kinase. Rho kinase inhibits PP1 $\delta$  (the catalytic subunit of MLCP) by phosphorylating MYPT1 (the myosin binding subunit of MLCP) at Thr-696 and Thr-853 residues. Thus, inhibition of either MLCK or RhoA-Rho kinase axis promotes MLC dephosphorylation and thus leads to reduced cell adhesion as a result of reduced contractility of the actin cytoskeleton. Because BAK leads to RhoA activation, the apparent MLC dephosphorylation can be attributed to direct inhibition of MLCK or a reduction in the phosphorylation potential as a result of ATP depletion.



or a decrease in the phosphorylation potential due to cellular ATP depletion.

A potential loss of MLCK activity cannot be attributed to the depletion of intracellular free  $\text{Ca}^{2+}$  ( $[\text{Ca}^{2+}]_i$ ), since BAK is likely to elevate  $[\text{Ca}^{2+}]_i$  through activation of nonselective cation channels.<sup>52</sup> However, direct effect on the activity of MLCK cannot be ruled out. As regards the intracellular ATP level, there is ample evidence for BAK-induced ATP depletion. Our results clearly show that the depletion could be due to a direct release of ATP (Fig. 7). Furthermore, deliberate ATP depletion by hypoxia and antimycin A treatment also led to MLC dephosphorylation similar to BAK treatment (Fig. 8).

In summary, BAK causes MLC dephosphorylation at concentrations lower than 0.005% in BCECs, possibly through the inhibition of MLCK and/or a reduced phosphorylation potential for activity of kinases concomitant with ATP loss. MLC dephosphorylation, which implies reduced actin contractility, could impair those cellular functions that contribute to the maintenance of the epithelial barrier. Further investigation is needed to demonstrate the significance of the findings in vivo.

## References

- Green K, Chapman JM. Benzalkonium chloride kinetics in young and adult albino and pigmented rabbit eyes. *J Toxicol Cutan Ocular Toxicol.* 1986;5:133-142.
- Gobbels M, Spitznas M. Corneal epithelial permeability of dry eyes before and after treatment with artificial tears. *Ophthalmology.* 1992;99:873-878.
- Lopez Bernal D, Ubels JL. Quantitative evaluation of the corneal epithelial barrier: effect of artificial tears and preservatives. *Curr Eye Res.* 1991;10:645-656.
- Ramselaar JA, Boot JP, van Haeringen NJ, et al. Corneal epithelial permeability after instillation of ophthalmic solutions containing local anaesthetics and preservatives. *Curr Eye Res.* 1988;7:947-950.
- Guo Y, Renner D, Begley C, Wilson G. Quantifying minor irritancy to the human corneal surface. *J Toxicol Cutan Ocular Toxicol.* 2003;22:147-155.
- Kovoor TA, Kim AS, McCulley JP, et al. Evaluation of the corneal effects of topical ophthalmic fluoroquinolones using in vivo confocal microscopy. *Eye Contact Lens.* 2004;30:90-94.
- Kossendrup D, Wiederholt M, Hoffmann F. Influence of cyclosporin A, dexamethasone, and benzalkonium chloride (BAK) on corneal epithelial wound healing in the rabbit and guinea pig eye. *Cornea.* 1985;4:177-181.
- O'Brien WJ, DeCarlo JD, Stern M, Hyndiuk RA. Effects of timoptic on corneal reepithelialization. *Arch Ophthalmol.* 1982;100:1331-1333.
- Tripathi BJ, Tripathi RC, Kolli SP. Cytotoxicity of ophthalmic preservatives on human corneal epithelium. *Lens Eye Toxicity Res.* 1992;9:361-375.
- Green K, Tonjum A. Influence of various agents on corneal permeability. *Am J Ophthalmol.* 1971;72:897-905.
- Pfister RR, Burstein N. The effects of ophthalmic drugs, vehicles, and preservatives on corneal epithelium: a scanning electron microscope study. *Invest Ophthalmol.* 1976;15:246-259.
- Tonjum AM. Effects of benzalkonium chloride upon the corneal epithelium studied with scanning electron microscopy. *Acta Ophthalmol.* 1975;53:358-366.
- Geerling G, Daniels JT, Dart JK, et al. Toxicity of natural tear substitutes in a fully defined culture model of human corneal epithelial cells. *Invest Ophthalmol Vis Sci.* 2001;42:948-956.
- De Saint Jean M, Debbasch C, Brignole F, et al. Toxicity of preserved and unpreserved antiglaucoma topical drugs in an in vitro model of conjunctival cells. *Curr Eye Res.* 2000;20:85-94.
- Xu KP, Li XF, Yu FS. Corneal organ culture model for assessing epithelial responses to surfactants. *Toxicol Sci.* 2000;58:306-314.
- De Saint Jean M, Brignole F, Bringuier AF, et al. Effects of benzalkonium chloride on growth and survival of Chang conjunctival cells. *Invest Ophthalmol Vis Sci.* 1999;40:619-630.
- Thoft RA, Friend J. The X, Y, Z hypothesis of corneal epithelial maintenance. *Invest Ophthalmol Vis Sci.* 1983;24:1442-1443.
- Satpathy M, Gallagher P, Jin Y, Srinivas SP. Extracellular ATP opposes thrombin-induced myosin light chain phosphorylation and loss of barrier integrity in corneal endothelial cells. *Exp Eye Res.* 2005;81:183-192.
- Garcia JG, Davis HW, Patterson CE. Regulation of endothelial cell gap formation and barrier dysfunction: role of myosin light chain phosphorylation. *J Cell Physiol.* 1995;163:510-522.
- Turner JR, Rill BK, Carlson SL, et al. Physiological regulation of epithelial tight junctions is associated with myosin light-chain phosphorylation. *Am J Physiol.* 1997;273:C1378-C1385.
- Turner JR. 'Putting the squeeze' on the tight junction: understanding cytoskeletal regulation. *Semin Cell Dev Biol.* 2000;11:301-308.
- Burridge K, Chrzanowska-Wodnicka M. Focal adhesions, contractility, and signaling. *Annu Rev Cell Dev Biol.* 1996;12:463-518.
- Ridley AJ. Rho family proteins: coordinating cell responses. *Trends in Cell Biology.* 2001;11:471-477.
- Ridley AJ. Rho GTPases and cell migration. *J Cell Sci.* 2001;114:2713-2722.

25. Fukata Y, Amano M, Kaibuchi K. Rho-Rho-kinase pathway in smooth muscle contraction and cytoskeletal reorganization of non-muscle cells. *Trends Pharmacol Sci.* 2001;22:32-39.
26. Kamm KE, Stull JT. Dedicated myosin light chain kinases with diverse cellular functions. *J Biol Chem.* 2001;276:4527-4530.
27. Ito M, Nakano T, Erdodi F, Hartshorne DJ. Myosin phosphatase: structure, regulation and function. *Mol Cell Biochem.* 2004;259:197-209.
28. Birukova AA, Smurova K, Birukov KG, et al. Microtubule disassembly induces cytoskeletal remodeling and lung vascular barrier dysfunction: role of Rho-dependent mechanisms. *J Cell Physiol.* 2004;201:55-70.
29. Hersch E, Huang J, Grider JR, Murthy KS. Gq/G13 signaling by ET-1 in smooth muscle: MYPT1 phosphorylation via ETA and CPI-17 dephosphorylation via ETB. *Am J Physiol.* 2004;287:C1209-C1218.
30. Sah VP, Seasholtz TM, Sagi SA, Brown JH. The role of Rho in G protein-coupled receptor signal transduction. *Annu Rev Pharmacol Toxicol.* 2000;40:459-489.
31. Satpathy M, Gallagher P, Lizotte-Waniewski M, Srinivas SP. Thrombin-induced phosphorylation of the regulatory light chain of myosin II in cultured bovine corneal endothelial cells. *Exp Eye Res.* 2004;79:477-486.
32. Essler M, Amano M, Kruse HJ, et al. Thrombin inactivates myosin light chain phosphatase via Rho and its target Rho kinase in human endothelial cells. *J Biol Chem.* 1998;273:21867-21874.
33. Garcia JG, Pavalko FM, Patterson CE. Vascular endothelial cell activation and permeability responses to thrombin. *Blood Coag Fibrinolysis.* 1995;6:609-626.
34. Seasholtz TM, Majumdar M, Kaplan DD, Brown JH. Rho and Rho kinase mediate thrombin-stimulated vascular smooth muscle cell DNA synthesis and migration. *Circ Res.* 1999;84:1186-1193.
35. Vouret-Craviari V, Boquet P, Pouyssegur J, Van Obberghen-Schilling E. Regulation of the actin cytoskeleton by thrombin in human endothelial cells: role of Rho proteins in endothelial barrier function. *Mol Biol Cell.* 1998;9:2639-2653.
36. van Hinsbergh VW, van Nieuw Amerongen GP. Intracellular signalling involved in modulating human endothelial barrier function. *J Anat.* 2002;200:549-560.
37. Somlyo AP, Somlyo AV. Signal transduction and regulation in smooth muscle [published correction appears in *Nature.* 1994;372:812]. *Nature.* 1994;372:231-236.
38. Ridley AJ, Hall A. The small GTP-binding protein rho regulates the assembly of focal adhesions and actin stress fibers in response to growth factors [see comment]. *Cell.* 1992;70:389-399.
39. Turner JR, Black ED, Ward J, et al. Transepithelial resistance can be regulated by the intestinal brush-border Na(+)/H(+) exchanger NHE3. *Am J Physiol.* 2000;279:C1918-C1924.
40. Chrzanowska-Wodnicka M, Burridge K. Rho-stimulated contractility drives the formation of stress fibers and focal adhesions. *J Cell Biol.* 1996;133:1403-1415.
41. Volberg T, Geiger B, Citi S, Bershadsky AD. Effect of protein kinase inhibitor H-7 on the contractility, integrity, and membrane anchorage of the microfilament system. *Cell Motil Cytoskeleton.* 1994;29:321-338.
42. Bacallao R, Garfinkel A, Monke S, et al. ATP depletion: a novel method to study junctional properties in epithelial tissues. I. Rearrangement of the actin cytoskeleton. *J Cell Sci.* 1994;107:3301-3313.
43. Patarca R, Rosenzwei JA, Zuniga AA, Fletcher MA. Benzalkonium salts: effects on G protein-mediated processes and surface membranes. *Crit Rev Oncog.* 2000;11:255-305.
44. Lang R, Song PI, Legat FJ, et al. Human corneal epithelial cells express functional PAR-1 and PAR-2. *Invest Ophthalmol Vis Sci.* 2003;44:99-105.
45. Lazar V, Garcia JG. A single human myosin light chain kinase gene (MLCK; MYLK). *Genomics.* 1999;57:256-267.
46. Lutz KL, Siahaan TJ. Molecular structure of the apical junction complex and its contribution to the paracellular barrier. *J Pharm Sci.* 1997;86:977-984.
47. Madara JL, Barenberg D, Carlson S. Effects of cytochalasin D on occluding junctions of intestinal absorptive cells: further evidence that the cytoskeleton may influence paracellular permeability and junctional charge selectivity. *J Cell Biol.* 1986;102:2125-2136.
48. Nybom P, Magnusson KE. Modulation of the junctional integrity by low or high concentrations of cytochalasin B and dihydrocytochalasin B is associated with distinct changes in F-actin and ZO-1. *Bioscience Rep.* 1996;16:313-326.
49. Stevenson BR, Begg DA. Concentration-dependent effects of cytochalasin D on tight junctions and actin filaments in MDCK epithelial cells. *J Cell Sci.* 1994;107:367-375.
50. Chahdi A, Daeffler L, Gies JP, Landry Y. Drugs interacting with G protein alpha subunits: selectivity and perspectives. *Fundam Clin Pharmacol.* 1998;12:121-132.
51. Debbasch C, Brignole F, Pisella PJ, et al. Quaternary ammoniums and other preservatives' contribution in oxidative stress and apoptosis on Chang conjunctival cells. *Invest Ophthalmol Vis Sci.* 2001;42:642-652.
52. Chang SW, Chi RF, Wu CC, Su MJ. Benzalkonium chloride and gentamicin cause a leak in corneal epithelial cell membrane. *Exp Eye Res.* 2000;71:3-10.
53. Allani PK, Sum T, Bhansali SG, et al. A comparative study of the effect of oxidative stress on the cytoskeleton in human cortical neurons. *Toxicol Appl Pharmacol.* 2004;196:29-36.
54. Banan A, Choudhary S, Zhang Y, et al. Oxidant-induced intestinal barrier disruption and its prevention by growth factors in a human colonic cell line: role of the microtubule cytoskeleton. *Free Radic Biol Med.* 2000;28:727-738.
55. Verin AD, Birukova A, Wang P, et al. Microtubule disassembly increases endothelial cell barrier dysfunction: role of MLC phosphorylation. *Am J Physiol.* 2001;281:L565-L574.
56. Szaszi K, Sirokmány G, Di Ciano-Oliveira C, et al. Depolarization induces Rho-Rho kinase-mediated myosin light chain phosphorylation in kidney tubular cells. *Am J Physiol.* 2005;289:C673-C685.